Catalysis Science & Technology

ROYAL SOCIETY OF CHEMISTRY

PAPER

View Article Online
View Journal | View Issue

Cite this: *Catal. Sci. Technol.*, 2025, 15, 6442

Phosphotungstic acid-supported alumina as a catalyst for glycerol monolaurate synthesis: process parameter optimization and reaction kinetics

Udit Khandara, [a] Verraboina Subbaramaiah [ab] and Vijayalakshmi Gosu *[a]

Received 22nd May 2025,
Accepted 4th September 2025

DOI: 10.1039/d5cy00612k

rsc.li/catalysis

Esterification of lauric acid with glycerol is an efficient way to valorize the excess glycerol produced as a by-product of biodiesel production. A phosphotungstic acid incorporated alumina (10HPW/Al_2O_3) catalyst was synthesized and employed as a heterogeneous catalyst for esterification of lauric acid with glycerol. The catalyst displayed potent catalytic activity even at a low catalyst dose of 0.5 wt%. The reaction temperature influenced catalytic activity as a two-fold increase in the conversion was observed with a rise in temperature from 403 K to 443 K. The catalyst showed catalytic activity for 4 reaction cycles without any substantial decrease in conversion. Kinetics models such as nucleophilic substitution (NS), Langmuir–Hinshelwood (LH) and Eley–Rideal (ER) models were investigated. Activation energy and pre-exponential factor for NS and LH models were calculated using the Arrhenius equation. Higher activation energy indicated that the mass transfer limitations were negligible for this catalyst. The synthesized catalysts can be used for up to 4 reaction cycles without any significant decline in the catalytic activity.

1. Introduction

The global biodiesel production rate is projected to increase up to 43.89 billion tons by 2030. However, despite its environmental advantages, the economic viability of biodiesel remains a significant challenge due to high feedstock costs and the accumulation of low-value by-product crude glycerol, which accounts for approximately 10 wt% of the total biodiesel output. Beyond the biodiesel industry, crude glycerol is also produced as a by-product in oleochemical manufacturing and soap production.[1] The surplus amount of crude glycerol has led to a substantial decline in market value that disrupts supply–demand dynamics and poses significant economic challenges for biodiesel producers. To enhance the economic feasibility of biodiesel production and promote sustainability, researchers have focused on the valorization of crude glycerol into high value and high-volume derivatives.

Among the various glycerol derivatives, glycerol monolaurate (GML) is one of the most versatile chemicals, with diverse industrial applications in cosmetics, healthcare, pharmaceuticals, food processing, and process industries.[2] GML can be synthesized through various pathways including esterification of lauric acid with glycerol in the presence of acidic catalysts (Fischer esterification),[3,4] transesterification of methyl laurate with glycerol 1,2-acetonide[5] and transesterification of methyl laurate with glycerol.[6] Among these routes, esterification of lauric acid with glycerol in the presence of acidic catalysts at moderate temperature (90–120 °C) is the most widely used commercial process.[7] The primary product, GML, can undergo consecutive esterification with excess lauric acid to form glycerol dilaurate (GDL), and subsequently, trace amounts of glycerol trilaurate (GTL).

In recent years, various homogeneous, enzyme-based, ionic liquid composites, and heterogeneous catalysts have been used for lauric acid esterification with glycerol. Enzymes like lipase offer high selectivity and mild conditions but face limitations such as high cost, low stability, and slow reactions.[8,9] Ionic liquid composites with heteropolyacids show promising properties but are inherently expensive and complex to prepare.[10] Homogeneous acid catalysts pose significant challenges associated with recyclability and recovery of the catalyst and require an additional separation and product purification process.[11] These drawbacks in homogeneous systems have shifted attention toward heterogeneous catalysts for their better recyclability, separation, and efficiency under mild conditions.

Various acid-based heterogeneous catalysts, such as organic/inorganic acid-modified mesoporous materials,[3] clay-

[a] *Department of Chemical Engineering, Malaviya National Institute of Technology, Jaipur-302017, India. E-mail: vlakshmi.chem@mnit.ac.in*
[b] *Department of Chemical and Life Science Engineering, Virginia Commonwealth University, Richmond, Virginia 23284, USA*

supported catalysts,[11] and resin-based catalysts,[12] have been widely utilized for the esterification of glycerol with lauric acid. Among these, heteropolyacids have emerged as promising catalytic materials owing to their high surface acidity, thermal and hydrolytic stability, and environmentally benign nature.[13] Heteropolyacids are ultra-strong Brønsted acids characterized by Keggin-type structures, which provide a high density of acidic sites and exhibit superior catalytic performance in various acid-catalyzed reactions. Notably, phosphotungstic acid (HPW) and silicotungstic acid supported catalysts have been investigated for the esterification of glycerol with lauric acid.[14,15] The use of supported HPW, especially on mesoporous materials, has shown good catalytic performance due to improved dispersion and stabilization of the active phase. However, despite their higher catalytic activity, the reusability of these catalysts has not been thoroughly explored. One of the major challenges associated with HPW based catalysts is the leaching of active HPW from the support in the presence of polar media, such as glycerol, which significantly diminishes catalytic performance. Consequently, the development of robust, recyclable HPA-based catalysts that can maintain higher catalytic activity in polar reaction environments remains an ongoing challenge.

Numerous studies have been conducted using various homogeneous and heterogeneous catalysts possessing Lewis acid sites. Lewis acid sites have been incorporated using calcium, magnesium, and cesium salts; however, these catalysts demonstrated limited stability, with poor recyclability. Few authors have made an attempt to enhance Lewis acid sites by incorporation of HPA on various support materials; these modifications have aimed to strengthen the interaction between the active HPA phase and the support material, thereby minimizing leaching and improving stability (Table 1).[13–16] Silver salt-modified HPAs have shown significantly improved stability, maintaining catalytic activity for up to 6 cycles.[13] Nevertheless, the use of silver salt limits its industrial applicability due to high cost.

To address these challenges, the present study explored the feasibility of phosphotungstic acid supported on alumina (Al_2O_3). Al_2O_3 is an attractive support material due to its widespread availability, low cost, and favorable physicochemical properties.[17] Furthermore, the HPW/Al_2O_3 catalyst has been employed in various acid-catalyzed processes, including esterification,[18] oxidative desulfurization of model fuel,[19] dehydration of ethanol to diethyl ether,[20] and *O*-alkylation of phenol using dimethyl ether.[21] The preparation of the HPW/Al_2O_3 catalyst is straightforward and economical compared to other supports such as SBA-15[22] and MCM-41.[3] The *x*HPW/Al_2O_3 catalyst exhibited enhanced structural integrity and resistance to leaching, even under harsh reaction conditions (polar reactants and elevated temperatures). Hence, the unique combination of stability, cost effectiveness, and facile preparation of the catalyst (HPW/Al_2O_3) presents an opportunity to assess its feasibility and performance to produce GML. Furthermore, no studies are available in the open literature for the production of GML using HPW/Al_2O_3.

The present study aimed to synthesize a highly acidic HPW incorporated alumina (HPW/Al_2O_3) catalyst for the esterification of glycerol with lauric acid. The synthesized catalyst was characterized using various techniques such as FTIR, XRD, XPS, BET, and FESEM-EDX to evaluate the structural, surface, and textural properties. The catalytic activity of the HPW/Al_2O_3 catalyst was investigated, and the process parameters associated with the esterification reaction were optimized to achieve the maximum yield of GML. Additionally, several kinetic models for the esterification reaction were proposed, and the kinetic parameters for the esterification of glycerol with lauric acid were evaluated. The stability of the HPW/Al_2O_3 catalyst was also assessed through its reusability study.

2. Experimental

2.1 Chemicals

Glycerol monolaurate was purchased from TCI Chemicals, India. Lauric acid (99% extra pure), glycerol (99%), phosphotungstic acid (HPW) and *n*-hexane (HPLC grade) were acquired from Loba Chemie Pvt. Ltd., India. Neutral alumina powder was procured from HPLC, India. HPLC grade methanol and acetone were procured from Thermo Fischer Scientific, India and Finar Chemicals, India, respectively.

Table 1 Performance of HPW based catalysts for esterification of lauric acid with glycerol

Catalyst	Modification	Operating conditions				GML yield (%)	Recyclability	Key findings	Ref.
		t	*T*	*m*	*M*				
20 wt% Cs-HPW/SBA-15	Cesium salt of tungstophosphoric acid supported on SBA-15	4	443	2.5	4 : 1	44.9	2	Catalyst did not display any signs of leaching up to 3 reaction cycles	16
20 wt% HPW/CaSBA-15	Functionalization of CaSBA-15 with HPW	6	—	—	—	55	2	Catalyst could be used for 2 recycling reactions	14
30 wt% HPW/MgSBA-15	Magnesium stabilized 12-tungstophosphoric acid impregnated SBA-15	6	433	3	4 : 1	55.35	2	No significant decline in LA conversion for two recycling reactions, but selectivity decreased as migration of some loosely bound HPW was induced by the formation of water	15
*x*HPW/Al_2O_3	HPW impregnated onto Al_2O_3	6	443	0.5	4 : 1	61.03	4	Highly stable catalyst up to 4 reaction cycles	Present study

2.2 Synthesis of catalysts (HPW supported on alumina)

Catalysts (5–30 wt% of HPW incorporated into alumina) were prepared *via* an impregnation method.[23] In a typical process, neutral alumina (Al_2O_3) was impregnated with the desired amount of HPW. Initially, the required amount of HPW was dissolved in distilled water. After that, the necessary amount of Al_2O_3 was added to the mixture. This mixture was stirred constantly for 35 hours at room temperature and then the mixture was dried at 373 K for 12 hours. The dried powder was calcined at 523 K for 5 hours. After calcination, the resultant catalyst was denoted as xHPW/Al_2O_3, where x refers to the amount of HPW loading in wt% of catalyst.

2.3 Characterization of xHPW/Al_2O_3

For identification of functional groups in the prepared catalyst, Fourier transform infrared (FTIR) spectra (PerkinElmer Massachusetts, USA) ranging from 4000–400 cm^{-1} were recorded in ATR mode. XRD spectral patterns were acquired using an X-ray diffractometer (PANalytical X'Pert, Netherlands) under Cu Kα radiation within the 2θ range from 5° to 90°. X-ray photoelectron spectroscopy (XPS) was performed using a Scienta Omicron spectrometer with an Al Kα source for investigation of the chemical state of the elements present in xHPW/Al_2O_3. The adsorption–desorption isotherm was obtained from nitrogen at 77 K using a BET-Chemisorption Analyzer (Anton Paar Autosorb iQ-C, Austria). Prior to this, the catalyst was degassed at 473 K for 3 hours. Brunauer–Emmett–Teller (BET) analysis was carried out to investigate the specific surface area of the catalyst. Using the Barrett–Joyner–Halenda (BJH) model, the pore size distribution of the prepared catalyst was derived. The internal morphology of the prepared catalyst was analyzed by high resolution transmission electron microscopy (HRTEM). The morphology of the prepared catalyst was characterized by Field emission scanning electron microscopy (FESEM) combined with energy dispersive X-ray (EDX) spectroscopy.

2.4 Esterification of lauric acid with glycerol

The catalytic performance of xHPW/Al_2O_3 was determined in a batch reactor (three neck round bottom flask) equipped with an oil bath on a hot plate magnetic stirrer (REMI 5 MLH Plus, India) to regulate the temperature and stirring. A Soxhlet apparatus combined with a glass coil condenser was employed. The reaction mixture consists of glycerol and lauric acid in a molar ratio of 4 : 1 and a known amount of catalyst was fed into the batch reactor. The reaction mixture was stirred at 1000 rpm and heated at 403 K for 6 hours.

After completion of the reaction, 20 μL of the upper layer consisting of lauric acid and products was taken and diluted with 400 μL of methanol. 5 μL of methyl acetate was used as an internal standard. This solution was analyzed using a high pressure liquid chromatograph (Thermo Scientific, Vanquish) equiped with C18 column (Hypersil GOLD™, 250 mm × 4.6 mm × 5 μm, Thermo Fischer Scientific™, Lithuania) combined with a diode array detector. The detection wavelength was set to 220 nm. 10% (by volume) *n*-hexane in methanol was used as a mobile phase for analysis with a flowrate of 0.5 mL min^{-1}. All the calculations were performed with lauric acid as the limiting reagent. Meanwhile, selectivity and yield were determined for glycerol monolaurate as the desired product. Turnover frequency (TOF) was calculated using HPW as the active site. The amount of HPW active sites of the spent catalyst through several reaction cycles was estimated *via* acid–base titration with a 0.01 N NaOH solution with a methyl orange solution as an indicator. Moles of desired product GML were estimated after 6 hours of reaction using GML yield and LA conversion.

$$\text{Conversion\%} = \frac{(\text{Initial moles of lauric acid}) - (\text{Final moles of lauric acid})}{(\text{Initial moles of lauric acid})} \times 100 \quad (1)$$

$$\text{Selectivity\%} = \frac{(\text{Moles of GML formed})}{(\text{Initial moles of lauric acid}) - (\text{Final moles of lauric acid})} \times 100 \quad (2)$$

$$\text{Yield\%} = \frac{(\text{Moles of GML formed})}{(\text{Initial moles of lauric acid})} \times 100 \quad (3)$$

$$\text{Turnover frequency} = \frac{(\text{Moles of desired product formed})}{(\text{Moles of active sites})(\text{Reaction time})} \quad (4)$$

Further, the optimization of associated process parameters was performed and the influence of each process parameter on the catalytic activity was evaluated using Pearson's correlation coefficient (PCC). The PCC matrix elements were in the range of −1 to 1, where −1 and 1 indicated strong negative and positive correlations, respectively, and PCC values approaching zero indicated no correlation. The reusability of the catalyst was investigated by separating the used catalyst from the reaction mixture. Initially, the upper organic phase containing lauric acid and reaction products was separated using methyl acetate, which is immiscible with glycerol. The lower phase, comprising glycerol and the solid catalyst, was then washed three times with 50 mL of methanol per step, maintaining a solid-to-liquid (S : L) ratio of approximately 20 : 1 (v/w). After each washing step, the mixture was centrifuged at 5000 rpm for 10 minutes to separate and recover the catalyst. The separated catalyst was washed and centrifuged several times to remove unwanted reactants and

products. The catalyst was dried at 373 K for removal of methanol. The dried catalyst was used for the next reaction cycle.

3. Results and discussion

3.1 Catalyst characterization

FTIR analysis of the alumina and prepared catalysts is depicted in Fig. 1. IR absorption peaks at ~3400 cm^{-1} and ~1600 cm^{-1} are attributed to the –OH vibrations and bending motions of H_2O molecules present in all samples.[24,25] For alumina, characteristic bands at ~600 cm^{-1} and ~800 cm^{-1} are associated with the Al–O vibrations.[25] The pure HPW exhibits characteristic peaks in the range of 650–1100 cm^{-1} corresponding to a previous study.[26] The stretching vibration band of P–O bonds associated with PO_4 and band corresponding to W=O bonds are present at ~1080 cm^{-1} and ~1000 cm^{-1}, respectively. Meanwhile, two P–O stretching vibration bands are weakly visible in the IR spectrum at ~1090 cm^{-1} due to the PO_4 present in the Keggin structure for catalysts with higher HPW loading (20% HPW/Al_2O_3 and 30% HPW/Al_2O_3), and disappeared from the IR spectra of the catalysts with lower HPW loading. This was attributed to the low content of $[PW_{12}O_{40}]^{3-}$ and lacunary $[PW_{11}O_{39}]^{7-}$.[26]

The XRD analysis of the 10HPW/Al_2O_3 catalyst and Al_2O_3 support provided vital information regarding the dispersion of HPW on the support surface. As depicted in Fig. 2, characteristic peaks of Al_2O_3 at ~37°, ~46°, and ~67° were attributed to the (131), (040) and (044) lattice planes, respectively.[21] The XRD spectrum signifies that the Al_2O_3 support has a poor crystalline structure which is suitable for the impregnation of HPW. The absence of characteristic peaks of HPW for 10HPW/Al_2O_3 signifies the uniform dispersion of HPW on the Al_2O_3 support.[21]

It is crucial that the support and the prepared catalyst have high specific surface area, appropriate pore volume and defined pore size to facilitate the esterification of lauric acid with glycerol. To investigate these physical properties, the nitrogen adsorption–desorption isotherm for the Al_2O_3 support and 10HPW/Al_2O_3 catalyst was measured along with the BJH pore size distribution (Fig. 3). The isotherm was type IV with a H_2 hysteresis loop in the relative pressure range of 0.4–1 and was related to capillary condensation in mesoporous support materials.[24] The BET surface area, pore volume, and average pore diameter of bare Al_2O_3 were 82 $m^2\ g^{-1}$, 0.246 cc g^{-1}, and 11.88 nm, respectively. This signifies that the HPW was dispersed on the surface as well as the pores of the support. After the impregnation of the HPW into the Al_2O_3 framework, the surface area and pore volume significantly decreased to 64.84 $m^2\ g^{-1}$ and 0.217 $cm^3\ g^{-1}$, respectively. However, the pore diameter increased to 13.42 nm which can be attributed to the collapse of smaller pores

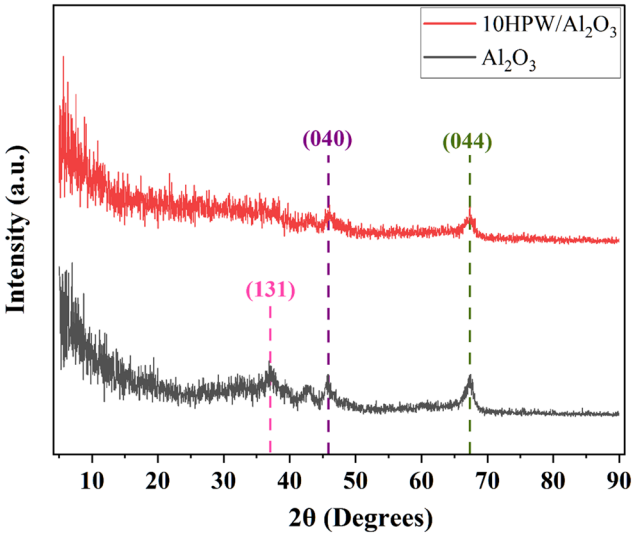

Fig. 2 XRD spectra of Al_2O_3 and 10HPW/Al_2O_3.

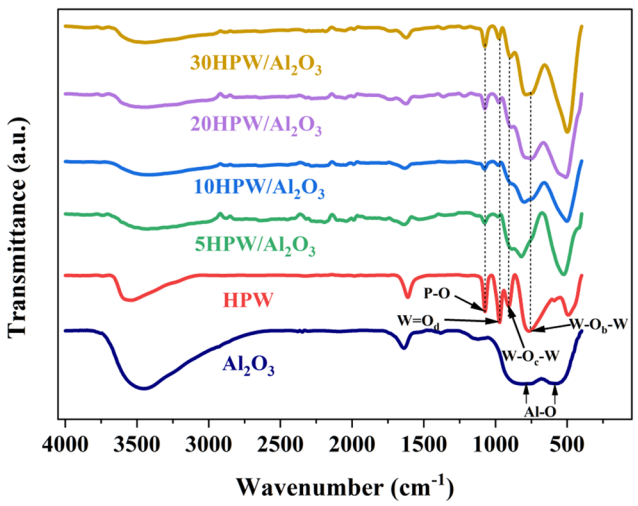

Fig. 1 FTIR spectra of alumina and the prepared catalysts.

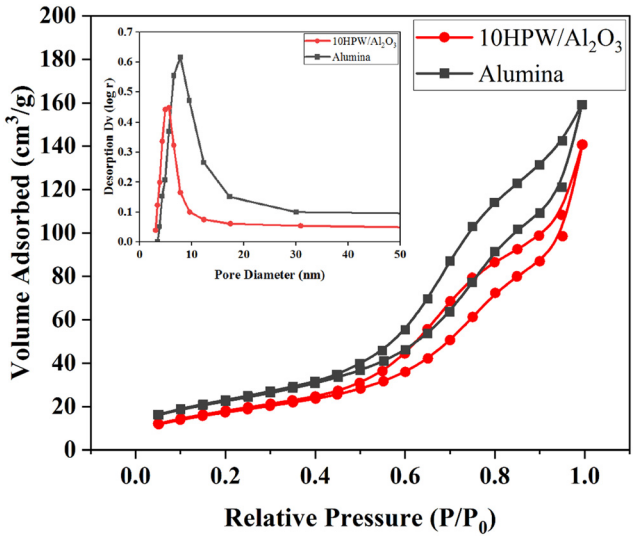

Fig. 3 Nitrogen adsorption–desorption isotherm and BJH pore size distribution (inset).

Table 2 Structural analysis and composition of the support and prepared catalyst

Sample	BET surface area[a] ($m^2\ g^{-1}$)	Pore volume[b] ($cc\ g^{-1}$)	Average pore diameter[b] (nm)
Al_2O_3	82.82	0.246	11.88
$10HPW/Al_2O_3$	64.84	0.217	13.42

[a] From the BET desorption method. [b] From the BJH desorption method.

to form larger pores[27] and partial deformation of the support structure.[19]

The BET specific surface area, average pore diameter and total pore volume are displayed in Table 2.

The XPS analysis of $10HPW/Al_2O_3$ and the alumina support was carried out to investigate the interactions between the elements of HPW and Al_2O_3 and is depicted in Fig. 4. XPS spectral peaks for Al 2p and O 1s were obtained at characteristic binding energies of 74 and 532 eV, respectively. The presence of W species can be verified through characteristic peaks of W 4f in the range of 36–38 eV (Fig. 4a). The XPS spectra of the W 4f peak was deconvoluted to W^{6+} and W^{5+} species at a binding energy of 38 and 36 eV, respectively (Fig. 4d).[28] A slight shift to higher binding energies in the XPS spectra of Al 2p (Fig. 4b) and O 1s (Fig. 4c) for the $10HPW/Al_2O_3$ catalyst indicates a potential interaction between HPW and the alumina support, which suggests a modification in the electronic environment of the surface species.[21]

The morphology of the prepared catalyst and alumina support was investigated using SEM-EDX (Fig. 5a and b).

The morphology of the alumina support contained well-defined cracks; meanwhile the $10HPW/Al_2O_3$ structure was observed to be spongy with several sheet-like structures on the surface.[21] No agglomeration of HPW was observed on the alumina. After the incorporation of HPW into Al_2O_3, a visible change in morphology was noticed. Moreover, the dispersion

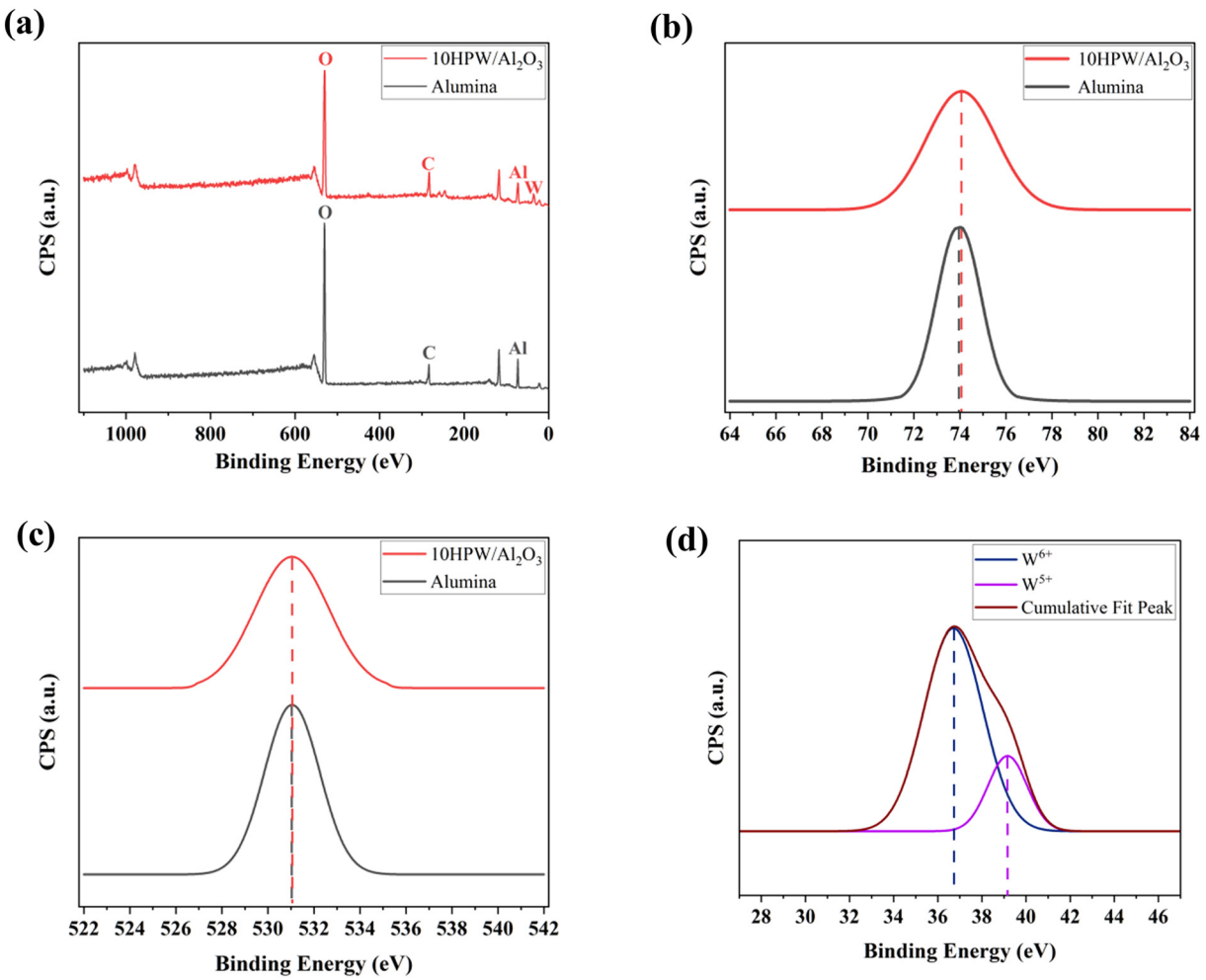

Fig. 4 XPS spectra of (a) $10HPW/Al_2O_3$ and alumina; (b) Al 2p; (c) O 1s; (d) W 4f.

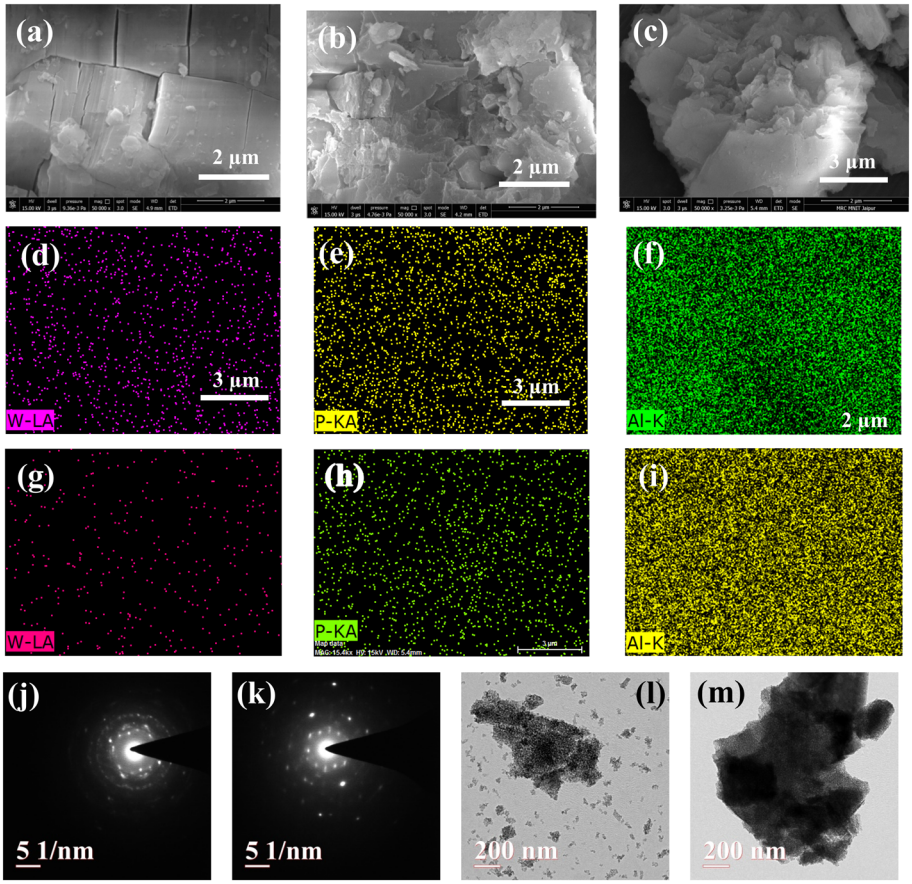

Fig. 5 Morphology of (a) Al_2O_3, (b) 10HPW/Al_2O_3 and (c) spent 10HPW/Al_2O_3. (d) Dispersion of W on 10HPW/Al_2O_3. (e) Dispersion of P on 10HPW/Al_2O_3. (f) Dispersion of Al on 10HPW/Al_2O_3. (g) Dispersion of W on spent 10HPW/Al_2O_3. (h) Dispersion of P on spent 10HPW/Al_2O_3. (i) Dispersion of Al on spent 10HPW/Al_2O_3. (j) SAED pattern of Al_2O_3. (k) SAED pattern of 10HPW/Al_2O. (l) TEM image of the Al_2O_3 support. (m) TEM image of 10HPW/Al_2O_3.

of various elements was investigated through EDX and is shown in Fig. 5d–f.

The elemental compositions of the alumina support, 10HPW/Al_2O_3 and spent 10HPW/Al_2O_3 are tabulated in Table 3. EDX analysis confirms the uniform dispersion of HPW species (W and P) on the catalyst support. The morphology of the spent catalyst remained similar to the fresh catalyst. Drastic reduction in the amount of W species was observed (Fig. 5g) due to leaching of active HPW into the reaction mixture after 4 reaction cycles.

High resolution transmission electron microscopy was used to gain insight about the internal morphology of the Al_2O_3 support and 10HPW/Al_2O_3 catalyst. The Selected Area Electron Diffraction (SAED) pattern confirms the polycrystalline structure of the alumina support and 10HPW/Al_2O_3 with concentric rings (Fig. 5j and k).[29] The presence of the Keggin structure is clearly visible in the TEM image of 10HPW/Al_2O_3 with distinct agglomeration of Keggin HPW on the Al_2O_3 support (Fig. 5l and m).

Table 3 Elemental composition of the support, fresh 10HPW/Al_2O_3 and spent 10HPW/Al_2O_3

Sample	Elemental composition[a] (atomic%)		
	Al	W	P
Al_2O_3	100.00	—	—
Fresh 10HPW/Al_2O_3	82.89	16.42	0.68
Spent 10HPW/Al_2O_3 (after 1 cycle)	88.25	9.98	2.15
Spent 10HPW/Al_2O_3 (after 2 cycles)	88.74	9.58	1.90
Spent 10HPW/Al_2O_3 (after 3 cycles)	88.42	9.35	1.59
Spent 10HPW/Al_2O_3 (after 4 cycles)	93.99	5.46	0.53

[a] From EDX analysis neglecting the amount of elements O and P.

3.2 Catalytic performance of *x*HPW/Al_2O_3

The synthesis of GML *via* esterification of lauric acid with glycerol is a Fischer esterification reaction and prominently influenced by operating parameters such as catalyst loading, catalyst dose, glycerol to lauric acid molar ratio, reaction temperature and reaction time. Therefore, the optimization of operating parameters was carried out to maximize the conversion of lauric acid, yield of GML and selectivity of GML. The influence of each parameter process was discussed elaborately in the subsequent section.

3.2.1 Influence of catalyst loading. Catalysts with different amounts of HPW loading (0–30 wt%) were tested for the esterification of glycerol with lauric acid at a constant reaction temperature of 403 K, a glycerol to lauric acid molar ratio of 4 : 1 and a catalyst dose of 2 wt% of the total reaction mixture. The catalytic activity in terms of conversion, selectivity and yield for each catalyst is depicted in Fig. 6a. A maximum conversion of 80.3% was obtained for mere HPW as the catalyst, but the yield of GML was only 31.62% due to lower selectivity towards GML. Furthermore, the selectivity was improved for HPW/Al_2O_3 with the incorporation of HPW into the Al_2O_3 support. An increasing trend in conversion was observed for the conversion of lauric acid with an increase in HPW loading; a maximum conversion of 72.10% was achieved with 30% HPW/Al_2O_3. On the other hand, selectivity initially increased and declined at higher HPW loading (20 and 30 wt%) as more active sites favored the formation of GDL. There was an insignificant difference in the LA conversion with the increase in the HPW loading in the range of 10–30%. Such behavior may be attributed to the blockage of mesopores due to the excess amount of HPW crystallites and create hindrance for accessibility to active sites.[15] The substantial decrease in the selectivity with HPW loading (20 and 30 wt%) influences the yield negatively despite the consistent increase in the conversion. The PCC for catalyst loading was also estimated to be slightly negative for conversion and yield (−0.059 and −0.025, respectively) (Fig. 6d). The PCC for conversion and yield being closer to zero validates that the catalyst loading does not have any influence on the catalytic activity. Since there was no substantial increase in GML after 10 wt% HPW loading, 10HPW/Al_2O_3 was chosen as the optimal HPW loading.

3.2.2 Influence of catalyst dose. The catalyst dose of 10HPW/Al_2O_3 was varied from 0.1–15 wt% by keeping the other parameters constant and the results are shown in Fig. 6b. In the range of 0.1–1 wt% of catalyst dose, selectivity towards GML was increased and perceived a declined trend with a further increase in catalyst dose due to the formation of undesired products, glycerol dilaurate (GDL) and glycerol trilaurate (GTL). No significant change in the yield was observed after the increase in the catalyst dose of 0.5 wt% attributing to the decline in the selectivity at higher catalyst dose. Although a higher catalyst dose (15 wt%) resulted in increased conversion (73.65%), selectivity and yield towards GML decreased to 41.35% and 30.46%, respectively. This decline suggests that an excessive catalyst dose may promote

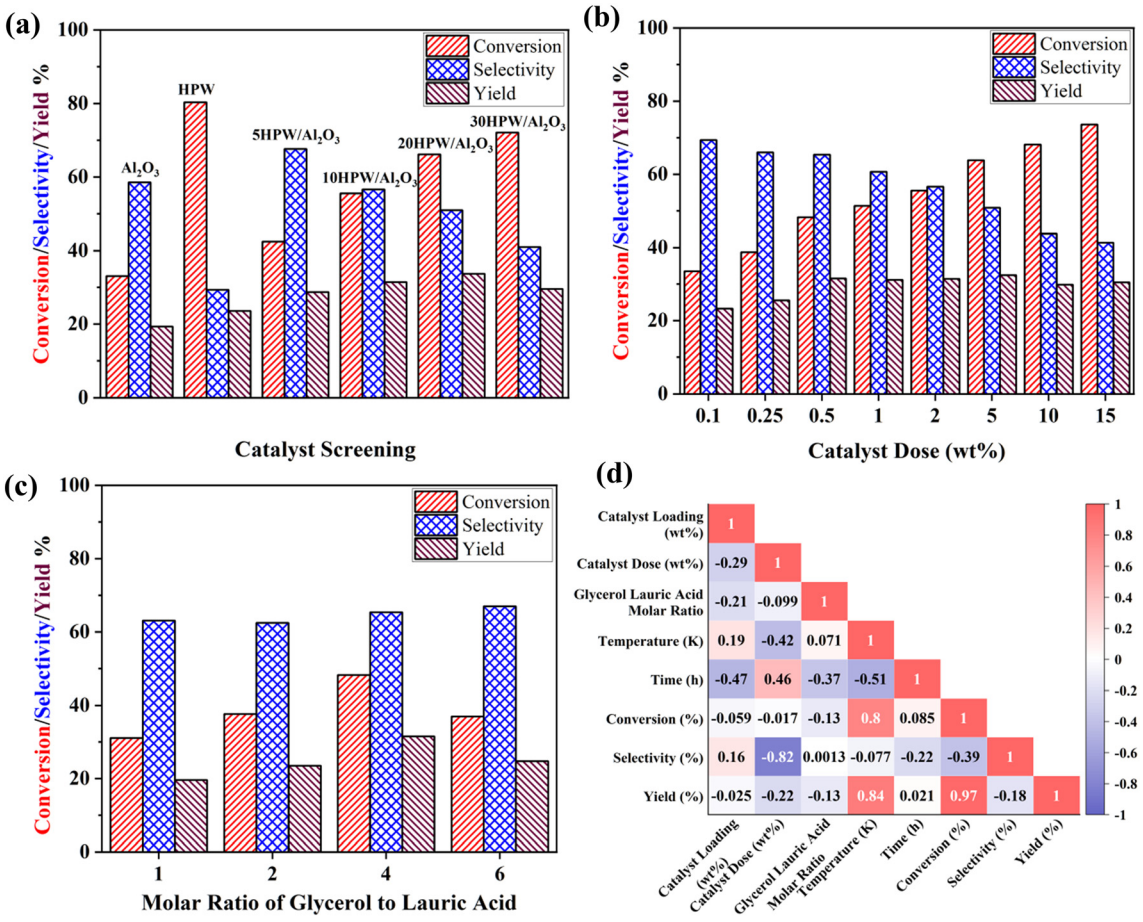

Fig. 6 Effect of (a) HPW loading, (b) catalyst dose and (c) molar ratio of glycerol to lauric acid on the catalytic activity of the HPW catalyst and (d) Pearson's correlation coefficient matrix for process parameters and catalytic activity.

secondary reactions that led to the formation of undesired by-products and reduce the overall efficiency of GML formation. The obtained trend is further verified by correlating catalyst dose with selectivity and the correlation was found to be inversely proportional with a PCC of −0.82 (Fig. 6d). Therefore, a catalyst dose of 0.5 wt% was considered as the optimal dose for the subsequent studies for which the highest yield of 31.52% was obtained.

3.2.3 Influence of glycerol to lauric acid molar ratio. The addition of excess glycerol accelerates the reaction rate towards the forward direction as per Le Chatelier's principle.[30] To maximize the GML formation the glycerol to lauric acid molar ratio varied from 1–6 at a reaction temperature of 403 K and a catalyst dose of 0.5 wt%. From Fig. 6c, it was clearly noticed that the increase in the molar ratio of glycerol in the reaction mixture led to a higher conversion and reached a maximum at a glycerol-to-lauric acid ratio of 4. However, a further increase in the molar ratio beyond 4 resulted in the dilution of the reaction mixture and the accumulation of excess glycerol on active sites, which inhibited the adsorption of lauric acid. The selectivity towards GML remained unaffected with an increase in the molar ratio, but reduced the conversion and yield. This trend was also validated by the PCC for glycerol to lauric acid molar ratio associated with catalytic activity. The PCC for selectivity was close to zero (0.0013), which means that the selectivity remains unaffected by the change in reactant molar ratio (Fig. 6d). Based on experimental results, the optimal glycerol-to-lauric acid molar ratio was found to be 4 and employed in the subsequent studies.

3.2.4 Influence of reaction temperature and reaction time. As per Arrhenius law, an exponential increase in the rate constant of a reaction can be achieved with an increase in the reaction temperature. The elevated reaction temperature even aids to minimize the mass transfer limitations and helps to achieve better interaction between reactants and active sites.[30] To improve the yield significantly, the reaction temperature was raised from 403–443 K while keeping all the optimized parameters constant. Furthermore, to account for the apparent effect of temperature on the esterification reaction, the reaction was carried out throughout a similar temperature range without the catalyst. This approach clarifies the true catalyst activity of the 10HPW/Al_2O_3 catalyst. The results are depicted in Fig. 7a–f in terms of conversion, selectivity and yield.

The significant increase in the conversion was observed at higher reaction temperature. Conversion rose substantially with an increase in the temperature. A two-fold increase in the conversion was achieved as the reaction temperature was raised from 403 to 443 K. This increase in the conversion at elevated temperature is accounted for by Arrhenius law which states the exponential influence of temperature on reaction kinetics. This significant difference in the conversion is attributed to readily available energy to overcome the activation energy barrier for more reactant molecules.[15] There was no significant change in selectivity towards GML throughout the reaction and this signifies the higher selectivity of the catalyst to facilitate the formation of GML at all the reaction temperatures. In the absence of catalyst, selectivity decreases substantially due to unhindered conversion of GML into glycerol dilaurate *via* further esterification with LA which is concerning. Since there was no effect of temperature was observed on the selectivity due to the narrow pore size distribution in the range of 2–10 nm, a mere increase in the conversion under the influence of temperature increase resulted in higher yield.[31] A maximum yield of 61.02% was achieved at 443 K after 6 hours of reaction with 96.81% conversion. This two fold increase in the conversion and yield suggest that the reaction temperature influences the catalytic activity dominantly in the presence of catalyst. In the absence of catalyst, even though 37.90% LA conversion was observed at 443 K after 6 hours of reaction, and due to a substantial decline in the selectivity, only 14.84% of GML yield was achieved.

This was further validated by correlating the reaction temperature and catalytic activity with conversion, selectivity and yield. The PCC for conversion and yield were estimated to be 0.8 and 0.84, respectively, which suggests a strong correlation (Fig. 6d). The PCC for selectivity was close to zero which would be appropriate as the selectivity does not change significantly with change in temperature. As there is no scope of increase in the conversion was perceived beyond 443 K, this temperature was considered the optimal temperature to maximize the GML yield.

3.3 Reusability of the 10HPW/Al_2O_3 catalyst

For economical production of GML, it is essential that the prepared catalyst sustains several cycles of reaction without any significant decline in the catalytic activity. As the highest yield was achieved at 443 K, the reusability study for 10HPW/Al_2O_3 was conducted at 443 K and is depicted in Fig. 8a. No significant reduction in the conversion was noticed up to cycle 5. This can be attributed to the strong interaction between HPW and the alumina support and its stability in polar reaction environments.[18] At cycle 5, the conversion was found to be 73.32%, with a yield of 48.1%. As no significant difference in the morphology was observed (Fig. 5c), this significant reduction in the activity could be attributed to the presence of active W species in the catalyst pores even though the SEM-EDX composition of W declined from the catalyst surface (Table 3). This trend is consistent with the catalytic performance in the esterification of lauric acid, where both lauric acid conversion and GML yield decreased in the fourth cycle. Furthermore, the TOF values calculated for each cycle indicate that the fresh catalyst exhibited a TOF of 2675.6 h^{-1}, which was sustained for 4 cycles by the catalyst. A further decline in TOF was observed for the fifth cycle with a TOF value of 2053.8 h^{-1} (Fig. 8b). The sustained value of TOF with each cycle is promising and reflects that esterification occurs inside the catalyst pores. Even though the amount of active sites from the surface is decreasing, the

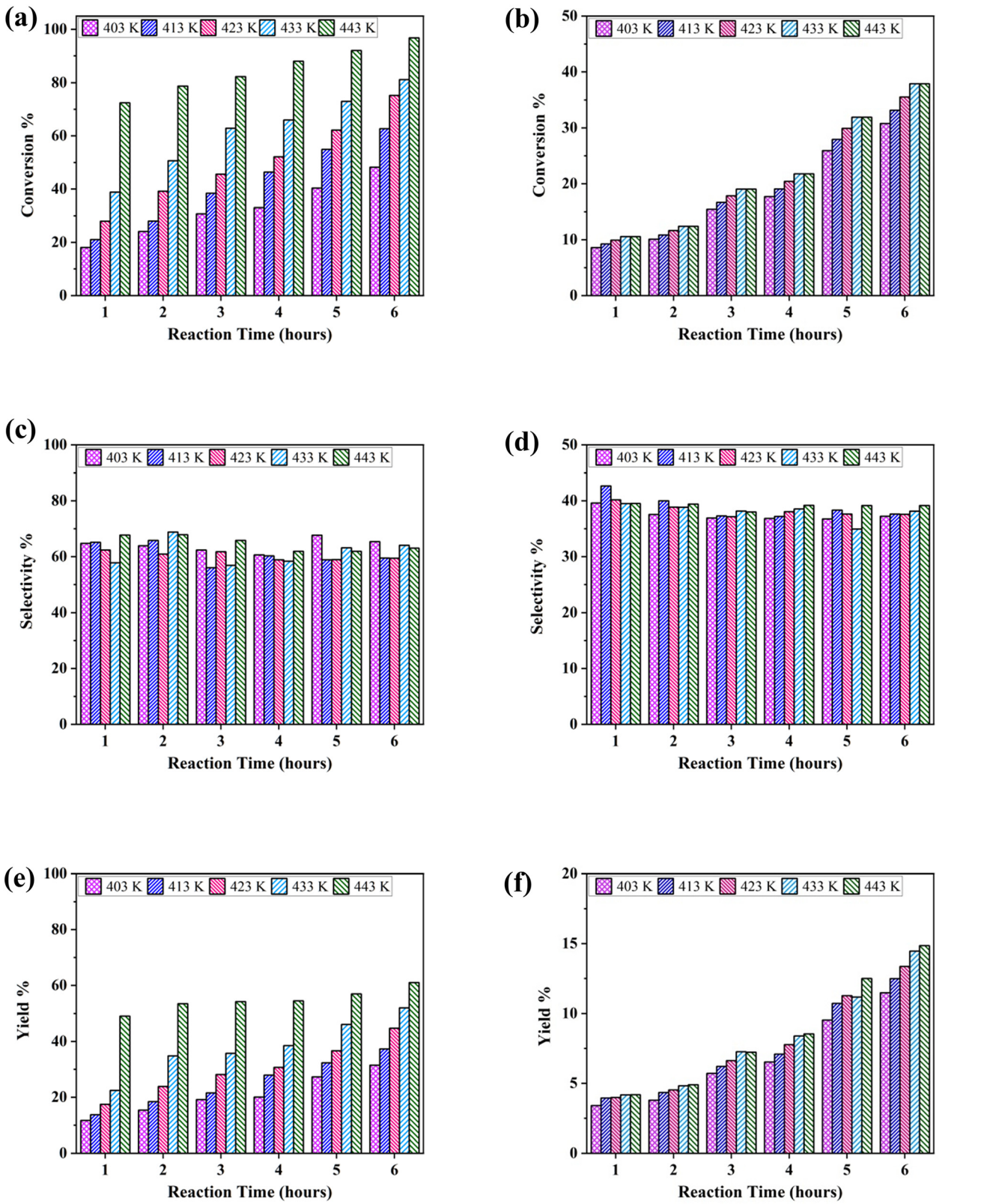

Fig. 7 Effect of reaction temperature on (a) LA conversion with catalyst, (b) LA conversion without catalyst, (c) GML selectivity with catalyst, (d) GML selectivity without catalyst, (e) GML yield with catalyst and (f) GML yield without catalyst.

conversion does not decline significantly. This phenomenon suggests the possibility of surface reaction inside catalyst pores. An *et al.*[32] estimated a turnover frequency of 209.5 h^{-1} for the Si (Ph–Ph)Si-ArSO_3H-HNS5.1 catalyst which was the

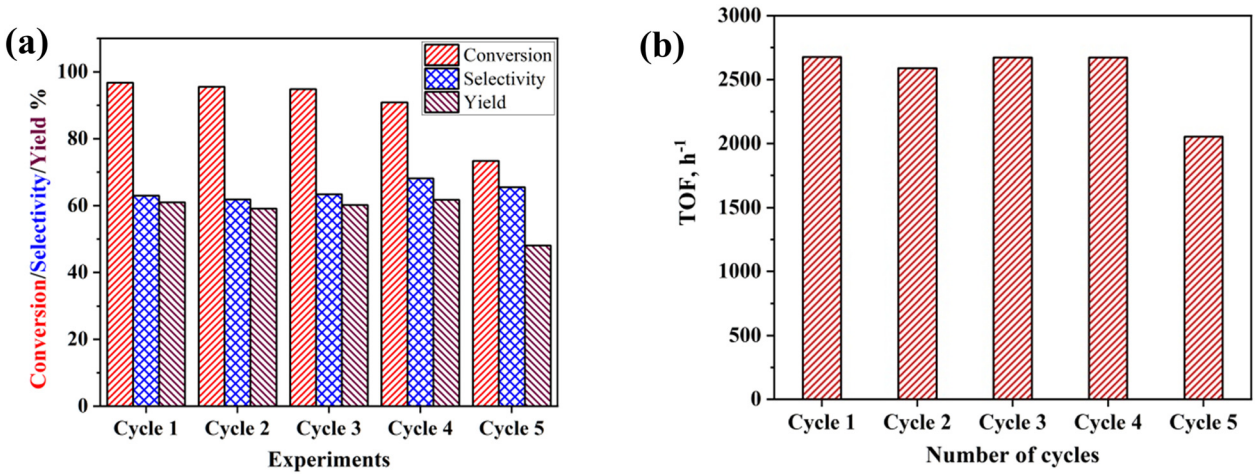

Fig. 8 (a) Reusability of 10HPW/Al_2O_3. (b) Turnover frequency for reaction cycles.

highest among all the solid catalysts investigated in the study. In another study, Sun *et al.*[33] reported a TOF value of 118.0 h^{-1} for the $[PrSO_3HN][SO_3CF_3]$/C-2 catalyst. The insignificant difference between turnover frequency (TOF) values indicates the presence of active sites in the catalyst pores which participate in the esterification. Therefore, the 10HPW/Al_2O_3 catalyst demonstrated stable performance for the esterification of glycerol with lauric acid up to four cycles (Fig. 8).

3.4 Kinetic modeling

Kinetic modeling is essential to provide insights into reaction mechanisms, catalytic performance and rate determining steps for the esterification of glycerol to lauric acid. In the present study, three kinetic models such as the nucleophilic substitution (NS) mechanism, Langmuir–Hinshelwood (LH) and Eley–Rideal (ER) were used to describe the kinetics of esterification of glycerol to lauric acid. The kinetic model equations and their assumptions are summarized in Table 4. Further, activation energy for the esterification of glycerol to lauric acid was calculated using rate constants (experimental) over a range of reaction temperatures (403–443 K).

For estimating kinetic data for the above-mentioned models, the esterification of lauric acid with glycerol was conducted in the range of reaction temperatures from 403–443 K and conversion was recorded hourly for a reaction time of 6 hours. The respective linear plots for each kinetic model and Arrhenius equation are depicted in Fig. 9.

Among all the kinetic models, the Eley–Rideal mechanism displayed a higher extent of deviation at higher temperature ranges (residual sum of squares = 206.32 at 443 K). The ER mechanism assumes that lauric acid adsorbs on the catalyst and reacts with bulk glycerol. The adsorption of lauric acid is exothermic which would hinder its adsorption at elevated temperatures. Furthermore, the ER mechanism also failed to accurately represent the reaction kinetics at higher temperatures. Conversely, NS and LH models represent the reaction kinetics linearly with negligible deviation. At elevated temperature, the model deviates slightly from the experimental kinetic data, but the R^2 values of 0.9616 and 0.9730 for LH and NS kinetic models are acceptable at 443 K, respectively. The kinetic model fits the experimental data with $R^2 > 0.96$ for both LH and NS kinetic models. On the other hand, Hoo *et al.*[34] reported the R^2 values of 0.4438 and 0.4923 for LH and NS kinetic models at 443 K, which

Table 4 Kinetic models, their assumptions and associated model equations[34,35]

Model	Equation	Assumptions
Nucleophilic substitution (NS)	$\ln\left(\frac{(R-X_A)}{R(1-X_A)}\right) = k_{NS}W(R-1)C_{A0}t$	• Esterification reaction is parallel and reversible • The protonation of lauric acid by glycerol attack is the only rate limiting step • By-product water is continuously removed from the reaction mixture
Langmuir–Hinshelwood (LH)	$(R-1)\ln\left(\frac{1}{1-X_A}\right) + X_A = \frac{k_{LH}W}{C_{A0}}t$	• Lauric acid adsorbs strongly onto the catalyst surface; meanwhile glycerol is adsorbed weakly • Esterification of lauric acid with glycerol is irreversible and the rate limiting step
Eley–Rideal (ER)	$\frac{X_A}{(1-X_A)} = k_T b_A C_{A0}\left[Wt - \ln\left(\frac{1}{1-X_A}\right)\right]$	• Only lauric acid is adsorbed onto the catalyst surface and covers the entire catalyst surface • Esterification of lauric acid with bulk glycerol is irreversible and the rate limiting step

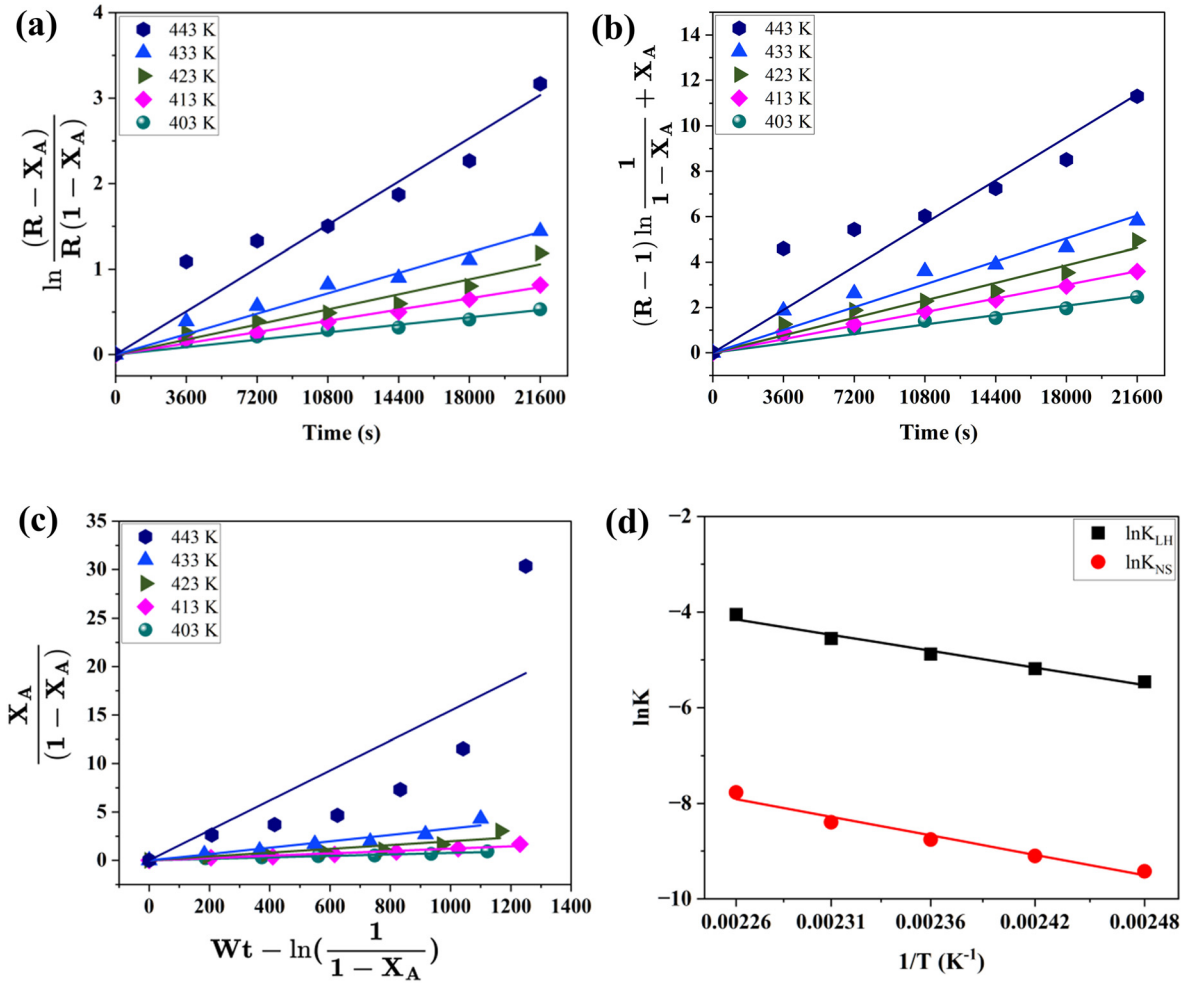

Fig. 9 Kinetics plots for (a) nucleophilic substitution, (b) Langmuir–Hinshelwood and (c) Eley–Rideal kinetic models; (d) Arrhenius plot for nucleophilic substitution and Langmuir–Hinshelwood kinetic models.

rendered the model fit subpar. This deviation was attributed to the formation of glycerol dilaurate and glycerol trilaurate *via* esterification of GML at elevated temperatures and desorption of lauric acid and glycerol from the catalyst surface.[34] The rate constant estimated using both models fits the Arrhenius plot with R_2 values of 0.9772 and 0.9714 for LH and NS models, respectively, which provides the suitable fitting at all temperature ranges even though the fitting is not satisfactory at elevated temperatures.

As observed in Fig. 7a, a thermally driven process is in effect here in addition to the catalytically driven process in terms of LA conversion. But, the assumptions taken for the development of kinetic models do not involve the inclusion of the thermally driven reaction process. As per authors' best knowledge, the LH and NS kinetic models do not account the effect of temperature as a separate term. The model accounts for the effect of temperature in terms of reaction rate constant.

The esterification reaction follows the NS mechanism with additional assumption that the glycerol is weakly adsorbed on the catalyst surface. This weakly adsorbed glycerol attacks on the protonated lauric acid.[34] The temperature dependence of reaction kinetics has been incorporated along with the reaction rate constant and has been calculated with the Arrhenius equation as shown in Table 5.

Chew *et al.*[35] reported the activation energy for an uncatalyzed reaction as 89.2 kJ mol^{-1}.[36] The incorporation of the *x*HPW/Al_2O_3 catalyst reduced the activation energy significantly and facilitated the formation of GML with higher selectivity towards GML. This indicates that the synthesized 10HPW/Al_2O_3 catalyst is a highly effective catalyst for GML synthesis *via* esterification of lauric acid with glycerol. The catalyst's selective pore structure was found to restrict the formation of larger by-products such as glycerol dilaurate (GDL) and glycerol trilaurate (GTL). The selective behavior can be attributed to the catalyst's tailored pore size that favors the formation of smaller GML molecules while minimizing the formation of undesired products. The influence of pore size on product selectivity has also been widely documented. Radhakrishnan *et al.*[31] put emphasis on the relationship between pore size and selectivity towards GML formation. The study estimated the cross-sectional

Table 5 Kinetics data calculation for NS and LH mechanisms

	Rate constant		R^2		Activation energy, E_a (kJ mol^{-1})		Pre-exponential factor, A	
T (K)	k_{NS}, 10^{-5} (L mol^{-1} g$_{cat}^{-1}$ s^{-1})	k_{LH}, 10^{-3} (mol L^{-1} g$_{cat}^{-1}$ s^{-1})	NS	LH	NS	LH	NS (L mol^{-1} g$_{cat}^{-1}$ s^{-1})	LH (mol L^{-1} g$_{cat}^{-1}$ s^{-1})
403	8.0967	4.255	0.9880	0.9845	59.22	51.06	3533.34	16 481.60
413	11.1571	5.602	0.9973	0.9964				
423	15.7491	7.607	0.9845	0.9875				
433	22.6278	10.536	0.9899	0.9824				
443	42.1519	17.439	0.9769	0.9671				

width of glycerol monolaurate and glycerol dilaurate as 0.8 and 1.0 nm, respectively. The higher selectivity towards GML formation was reasoned with constraint of pore size. Further, the higher selectivity was attributed to the narrow pore size distribution within the catalyst.[31] Similarly, Wibowo *et al.*[37] deemed the stearic effect within the pores an influential factor favoring the GML formation. The study reported higher GML selectivity for the TBMMT catalyst having a pore size of 14.0 nm. The current study also reports the average pore diameter of 13.42 nm, which could be the reason for higher GML selectivity. Similar observations were made by Abdullah *et al.*[3] and further support the influence of pore size distribution over GML selectivity.

In heterogeneous catalysis, the overall reaction rate may be limited either by bulk diffusion or pore diffusion. To evaluate the possible influence of internal (pore) diffusion, the Weisz–Prater criterion was applied for the esterification of lauric acid with glycerol over the phosphotungstic acid supported alumina (10HPW/Al_2O_3) catalyst.[38] According to the Weisz–Prater (C_{WP}) criterion, values of $C_{WP} \gg 1$ indicate strong internal diffusion limitations, whereas C_{WP} values $\ll 1$ confirm that the reaction is controlled by surface reaction kinetics rather than pore diffusion.

The Weisz–Prater number is defined as:

$$C_{WP} = \frac{(-r)\rho_c R^2}{D_i C}$$

where $(-r)$ is the average reaction rate per unit catalyst weight (calculated for both glycerol and lauric acid), ρ_c is the catalyst density, R is the average catalyst particle radius, C is the reactant concentration, and D_i is the self-diffusion coefficient of the reactant.

In this study, the average particle radius (R) was estimated to be ~5 μm and the catalyst density (ρ_c) was taken as 0.981 g cm^{-3}. The self-diffusion coefficients were taken as ~2.5 × 10^{-10} m^2 s^{-1} for glycerol[39] and ~3.75 × 10^{-10} m^2 s^{-1} for lauric acid[40] (literature values).

The calculated C_{WP} values were 1.40 × 10^{-3} and 1.44 × 10^{-3} for glycerol and lauric acid, respectively. Since both values are significantly smaller than 1, the results clearly indicate that the esterification reaction is not limited by internal mass transfer, and the kinetics are governed primarily by the surface reaction. Furthermore, previous reports have shown that catalysts with small particle sizes and pore diameters larger than 4 nm generally exhibit negligible mass transfer limitations, which supports our findings.[42]

Additionally, the higher energy activation values for both kinetic models suggest that the reaction is insignificantly affected with mass transfer limitations. Instead, the reaction appears to be primarily controlled by the surface interaction between lauric acid and glycerol. The effect of mass transfer was investigated by Hu *et al.*,[41] using different stirring speeds in the range of 300–1100 rpm. The effect of different stirring speeds was found to be negligible and the effect of mass transfer was deemed to be eliminated. In the case of heterogeneous reaction in the presence of a solid catalyst, the process consists of transfer of the reactant from the bulk to active sites in the internal pores of the catalyst. After the reaction at the active sites in the pores, the products diffuse out of internal pores into the bulk. In the case of reactions that demand higher activation energy, the surface reaction shows far more resistance in comparison to other steps, which involve mass transfer from the bulk to active sites and *vice versa*. In contrast, reactions with lower activation energy requirement are very fast and resistance for the surface reaction is minimal, which renders the mass transfer steps slow and controlling. The correlation between the mass transfer limitation and activation energy has been reported by several studies subsequently. Chew *et al.*[35] demonstrated that in the case of esterification, activation energy higher than 25 kJ mol^{-1} indicates that the reaction is truly limited by the surface reaction step and mass transfer limitations are negligible. Thus, the surface reaction is found to be the rate-limiting step, which is consistent with the literature.[42]

4. Conclusion

The present study synthesized a phosphotungstic acid incorporated alumina (HPW/Al_2O_3) catalyst and employed for esterification of lauric acid with glycerol to produce GML. The synthesized catalyst was crystalline in nature with a narrow pore size distribution, attributed to the high selectivity towards GML formation. The BET surface area of the catalyst was found to be 64.84 m^2 g^{-1} with pore diameter in the range of 2–10 nm. The HPW species were uniformly distributed over the catalyst surface without any agglomeration. The highest GML yield of 61.03% was achieved at 443 K with a 96.81% conversion using

0.5 wt% of 10HPW/Al_2O_3 and a glycerol-to-lauric acid ratio of 4, accompanied by approximately 28% GDL. Trace amounts of GTL were also detected but were considered negligible for quantification. The *x*HPW/Al_2O_3 catalyst exhibited enhanced structural integrity and resistance to leaching, even under harsh reaction conditions (polar reactants and elevated temperatures). Furthermore, the catalyst demonstrated sustained catalytic activity across four consecutive esterification cycles, thereby exceeding the recyclability and stability typically observed in HPW-based catalysts. Therefore, *x*HPW/Al_2O_3 emerges as a practically robust and economically viable catalyst for sustainable industrial processes. The catalyst was highly selective towards the formation of GML due to the fine pore size distribution in the range of 2–10 nm. Among all the process parameters, the reaction temperature was found to be crucial as the conversion increased two-fold (96.81% at 443 K compared to 48.22% at 403 K). The prepared catalysts also displayed exceptional stability under harsh reaction conditions as they could facilitate the reaction for 4 cycles without a significant decrease in the catalytic activity. Furthermore, the three kinetic models such as the nucleophilic substitution mechanism, Langmuir–Hinshelwood mechanism and Eley–Rideal mechanism were employed at different reaction temperatures. Among these kinetic models, Eley–Rideal could not accurately represent the reaction kinetics at high temperature ranges. Kinetic parameters such as activation energy and pre-exponential factor were estimated for best fitted kinetic models (nucleophilic substitution and Langmuir–Hinshelwood) using the Arrhenius equation. The surface reaction was supposed to be the rate limiting step due to higher activation energies and mass transfer limitations were found to be negligible. Therefore, the findings of the current study confirm that the synthesized catalyst has potential to enhance GML production and contribute to the sustainable growth of the biodiesel industry.

Conflicts of interest

The authors declare that they have no known competing financial interests or personal relationships that could have appeared to influence the work reported in this paper.

Data availability

The data that support the findings of this study are available from the corresponding author upon reasonable request.

Acknowledgements

The authors acknowledge the Ministry of Education (MoE), Government of India and Malaviya National Institute of Technology, Jaipur for providing financial support.

References

1 M. Ayoub and A. Z. Abdullah, *Renewable Sustainable Energy Rev.*, 2012, **16**, 2671–2686.
2 A. Mustafa, F. Niikura, C. Pastore, H. A. Allam, O. B. Hassan, M. Mustafa, A. Inayat, S. A. Salah, A. A. Salam and R. Mohsen, *Sustainable Chem. Pharm.*, 2022, **27**, 100690.
3 A. Z. Abdullah, N. Ghazali, P. Y. Hoo and N. I. Basir, *Chem. Eng. Commun.*, 2021, **209**, 607–622.
4 Z. Shen, L. Chen, H. Cheng and Z. Qi, *Catal. Today*, 2021, **407**, 291–300.
5 F. O. Nitbani, L. S. Angwarmasse, E. Y. Bessy, H. E. Wogo, A. I. R. Detha and P. J. P. Tjitda, *J. Oleo Sci.*, 2022, **71**, 1013–1020.
6 N. N. A. Jamlus, J. Salimon and D. Derawi, *Malays. J. Anal. Sci.*, 2016, **20**, 1365–1372.
7 A. Mustafa, S. Fathy, O. Kutlu, F. Niikura, A. Inayat, M. Mustafa, T. M. M. Abdellatief, A. Bokhari, O. D. Samuel, C. Pastore, L. di Bitonto, M. A. Tawfik, M. Munir and R. Mohsen, *Clean Technol. Environ. Policy*, 2023, **25**, 3263–3283.
8 B. Zha, Z. Chen, L. Wang, R. Wang, Z. Chen and L. Zheng, *Eur. J. Lipid Sci. Technol.*, 2014, **116**, 328–335.
9 C. C. B. Pereira, M. A. P. Da Silva and M. A. P. Langone, *Appl. Biochem. Biotechnol.*, 2004, **114**, 433–445.
10 X. Han, X. Zhang, G. Zhu, J. Liang, X. Cao, R. Kan, C. Te Hung, L. L. Liu and S. Bin Liu, *ChemCatChem*, 2017, **9**, 2727–2738.
11 A. Z. Abdullah, T. Y. Wibowo and R. Zakaria, *Chem. Eng. J.*, 2011, **167**, 328–334.
12 Y. Pouilloux, S. Abro, C. Vanhove and J. Barrault, *J. Mol. Catal. A: Chem.*, 1999, **149**, 243–254.
13 C. Xu, J. Gan, X. Mei, Y. Zhou, J. Duanmu, G. Zhu, H. Zhang, X. Han, Y. Wang and S. Bin Liu, *Catal. Lett.*, 2020, **150**, 3584–3597.
14 P. Hoo, A. Z. Abdullah, S. H. Shuit, Y. P. Teoh, Q. H. Ng and B. Kunasundari, *IOP Conf. Ser.: Mater. Sci. Eng.*, 2018, **318**(1), DOI: **10.1088/1757-899X/318/1/012007**.
15 S. Y. Ooi, P. Yong, A. Zuhairi, S. Kartini and E. Ab, *S. Afr. J. Chem. Eng.*, 2022, **41**, 51–64.
16 S. N. M. Saleh, M. Hizami, M. Yusoff and A. Z. Abdullah, *Arabian J. Sci. Eng.*, 2018, **43**, 5771–5783.
17 Y. Zhang, B. Huang, M. K. Mardkhe and B. F. Woodfield, *Microporous Mesoporous Mater.*, 2019, **284**, 60–68.
18 P. Nazari and S. R. Setayesh, *Can. J. Chem. Eng.*, 2018, **96**, 1176–1184.
19 X. Yan, L. Xiong and P. Mei, *J. Wuhan Univ. Technol., Mater. Sci. Ed.*, 2014, **29**, 237–241.
20 A. E. A. A. Said, M. M. M. Abd El-Wahab and M. M. Abdelhak, *React. Kinet., Mech. Catal.*, 2017, **122**, 433–449.
21 M. Samruddhi, A. Bhatkar, M. Prabu, S. P. Mekala, P. Gogoi, G. Mohapatra and R. Thirumalaiswamy, *Reactions*, 2022, **3**, 602–614.
22 P. Hoo and A. Z. Abdullah, *Korean J. Chem. Eng.*, 2016, **33**, 1200–1210.
23 P. Sharma, S. Vyas and A. Patel, *J. Mol. Catal. A: Chem.*, 2004, **214**, 281–286.
24 L. R. V. Da Conceição, C. E. R. Reis, R. De Lima, D. V. Cortez and H. F. De Castro, *RSC Adv.*, 2019, **9**, 23450–23458.
25 H. K. Wang, C. Y. Yi, L. Tian, W. J. Wang, J. Fang, J. H. Zhao and W. G. Shen, *J. Nanomater.*, 2012, **2012**, 453915.

26 G. S. Armatas, A. P. Katsoulidis, D. E. Petrakis and P. J. Pomonis, *J. Mater. Chem.*, 2010, **20**, 8631–8638.
27 L. Gavrilović, S. S. Kazi, A. Nelson, A. G. P. Oliveira and J. Meyer, *Catal. Commun.*, 2023, **185**, 106800.
28 S. Chen, L. Lin, X. Jing and Y. Yang, *ChemistrySelect*, 2019, **4**, 4854–4860.
29 A. Alinda Shaly, G. Hannah Priya, M. Mahendiran, J. Mary Linet and J. Arul Martin Mani, *Phys. B*, 2022, **642**, 414100.
30 U. Khandara, V. Subbaramaiah and V. Gosu, *Chem. Eng. J.*, 2024, **488**, 150938.
31 R. Radhakrishnan, J. Wu, S. Jaenicke and G. K. Chuah, *ChemCatChem*, 2011, **3**, 761–770.
32 S. An, Y. Sun, D. Song, Q. Zhang, Y. Guo and Q. Shang, *J. Catal.*, 2016, **342**, 40–54.
33 Y. Sun, J. Hu, S. An, Q. Zhang, Y. Guo, D. Song and Q. Shang, *Fuel*, 2017, **207**, 136–145.
34 P. Hoo and A. Z. Abdullah, *Ind. Eng. Chem. Res.*, 2015, **54**, 7852–7858.
35 S. J. Chew, P. Y. Hoo, A. Z. Abdullah, S. K. E. A. Rahim, Y. P. Teoh, S. H. Shuit and Q. H. Ng, *AIP Conf. Proc.*, 2022, **2496**, DOI: **10.1063/5.0090713**.
36 L. Hermida, A. Z. Abdullah and A. R. Mohamed, *Chem. Eng. J.*, 2011, **174**, 668–676.
37 T. Y. Wibowo, A. Z. Abdullah and R. Zakaria, *Appl. Clay Sci.*, 2010, **50**, 280–281.
38 C. D'Agostino, Y. Ryabenkova, P. J. Miedziak, S. H. Taylor, G. J. Hutchings, L. F. Gladden and M. D. Mantle, *Catal. Sci. Technol.*, 2014, **4**, 1313–1322.
39 M. Požar and B. Lovrinčević, *Soft Matter*, 2024, **20**, 8061–8067.
40 M. Iwahashi, S. Takebayashi, M. Taguchi, Y. Kasahara, H. Minami and H. Matsuzawa, *Chem. Phys. Lipids*, 2005, **133**, 113–124.
41 H.-Q. Hu, Y. Zhang, M. Fan, Y. Cai, G.-W. Chu and L.-L. Zhang, *Chin. J. Chem. Eng.*, 2024, **70**, 211–221.
42 V. Brahmkhatri and A. Patel, *Fuel*, 2012, **102**, 72–77.